Microelectronic Engineering 259 (2022) 111780

Contents lists available at ScienceDirect

Microelectronic Engineering

journal homepage: www.elsevier.com/locate/mee

Reactive ion etching of tantalum in silicon tetrachloride

Asaad K. Edaan Al-mashaal [a,*], Rebecca Cheung [b]

[a] Material Science Department, Polymer Research Centre, University of Basrah, Basrah 61004, Iraq
[b] School of Engineering, Institute for Integrated Micro and Nano Systems, University of Edinburgh, Edinburgh EH9 3FF, United Kingdom

ARTICLE INFO

Keywords:
Reactive ion etching
Silicon tetrachloride
Plasma etching
Tantalum

ABSTRACT

A precise patterning of metal structures plays an essential role in the development of feasible metal-based devices. By examining the etching conditions under which a layer of material is properly etched, the etching process can be further optimised and hence controlled. This work reports on the reactive ion etching (RIE) of micrometric films of tantalum (Ta) using silicon tetrachloride ($SiCl_4$)/Argon (Ar) plasmas. The etching characteristics have been studied with respect to $SiCl_4$/Ar ratio, plasma power and chamber pressure. It has been found that increasing the flow rate of $SiCl_4$ or plasma power leads to an increase in the etching rate. Moreover, the observations suggest that it is ineffective to increase the flow rate of Ar to more than 30 sccm and the plasma pressure to more than 100 mTorr. The work implemented here represents an important step for the development of tantalum-based structures that can be used in a wide range of devices.

1. Introduction

The selection of materials used in integrated circuits and microelectromechanical systems (MEMS) has broadened considerably in recent years. With the advancement in manufacturing technologies, electronic and electromechanical devices now involve not only semiconductors but also incorporate other materials such as metals, insulators and polymers. Refractory metals possess outstanding characteristics that have been a topic of significant interest [1]. Tantalum (Ta) is one of the refractory metals that has attracted research and industrial attention over many years due to its excellent physical and chemical properties such as high melting point, high mechanical strength, biocompatibility and high wear resistance [2]. Such characteristics would make tantalum a suitable material for several applications, including but not restricted to biomedical implants [3], MEMS-based sensors and resonators [4–7], biomimetic systems [8] resonant gate transistors [8,9], protective coatings [10–12] and diffusion barriers [13,14].

In order to use tantalum in the intended application, especially in electronics and MEMS devices, it must be etched/patterned in such a way that leads to precisely fabricated structures. Tantalum metal, however, is well known for its remarkable corrosion resistance and chemical inertness [15,16]. Such features make tantalum immune to chemical attack in most hydrous media. The solutions that are found to etch tantalum are hydrofluoric (HF) acid, sulfuric acid (H_2SO_4), free sulphur trioxides (SO_3), nitric acid (HNO_3) and fluoride ions [15–19]. However, the wet etch process suffers from several drawbacks, the most important of which are safety (due to the corrosion of acids), undercutting that results from the isotropic etching [20,21] and possibly damage to other layers attacked by wet etchants. More importantly, devices that rely on suspended mechanical components, a sacrificial layer must be applied first and then etched away to release the final structure [20]. Nevertheless, if a wet-based etching process is used for the release, stiction-related problems are encountered in the final structure. Such stiction issues could prevent the device from working properly. It appears, therefore, that wet etching is not always the preferred technique to etch tantalum for MEMS and microelectronics applications.

Based on the challenges in obtaining reliably defined patterns of tantalum using wet etching methods, it is vital to employ an alternative etching process. Different dry etching techniques have been developed to etch tantalum. One of the dry etching approaches in which higher anisotropic etch profiles with vertical sidewalls can be obtained is reactive ion etching (RIE). The reactive ion etching of tantalum has been commonly carried out in fluorine- and chlorine-based plasmas. A number of studies have been reported on the reactive ion etching of tantalum

Abbreviations: Reactive Ion Etching, RIE; Tantalum, Ta; Silicon Tetrachloride, $SiCl_4$; Plasma, Pl; microelectromechanical systems, MEMS; Scanning electron microscopy, SEM; energy dispersive X-ray spectrometry, EDS.

* Corresponding author.
E-mail address: asaad.edaan@uobasrah.edu.iq (A.K. Edaan Al-mashaal).

https://doi.org/10.1016/j.mee.2022.111780
Received 16 February 2022; Accepted 7 April 2022
Available online 16 April 2022

using different mixtures of plasmas such as sulphur hexafluoride (SF_6) or SF_6/O_2 [22], chlorine (Cl_2)/chloroform ($CHCl_3$) [23,24], carbon tetrafluoride (CF_4) [25–28], trifluoromethyl chloride (CF_3Cl) and fluoroform (CHF_3) [28,29], CF_4/CHF_3 [30]. In addition, a Bosch-based deep reactive ion etching (DRIE) process has been utilised to etch tantalum in a plasma mixture of sulphur hexafluoride (SF_6) and octafluorocyclobutane (C_4F_8) [31]. Similarly, tantalum-based films have been etched using three mixtures of plasmas: hexafluoroethane (C_2F_6)/Ar, hydrogen bromide (HBr)/Ar and Cl_2/Ar [32]. Issues noticed in these etching studies include the relatively fast etch rate, undercutting, overetching, using hard mask instead of photoresist and complicated etching configuration. With relatively large etch rates of 6 μm/min or higher, the etching process might be uncontrollable and can affect the layers underneath, hence such etching recipes are not suitable for precisely controlled features.

In this work, a thoroughgoing investigation of the RIE characteristics of tantalum films in $SiCl_4$/Ar plasmas has been conducted. Plasma based on $SiCl_4$ has already been utilised to etch a number of materials such as gallium arsenide (GaAs) [33], gallium phosphide (GaP) [34], amorphous silicon (a-Si:H) and silicon nitride (SiN_x) [35]. $SiCl_4$ and nitrogen trifluoride (NF_3) plasmas have been used to etch tantalum and tantalum nitride [36]. Despite the high selectivity obtained, the work was limited to study the etching rate as a function of gas mix ratio without addressing the influence of other etching parameters such as power and pressure. Therefore, it is essential to dig deeper into the etching process and to select the appropriate etching recipe of tantalum. The purpose of the present study is to address the effect of the etching process conditions, namely the gas composition of $SiCl_4$/Ar mixture, pressure and power, on the etch rate of tantalum films. To the best of our knowledge, no previous work dealing with the etching of tantalum in $SiCl_4$/Ar has been conducted in such a comprehensive way. The outcomes of this study would be beneficial to the realisation of tantalum-based devices where fine and precisely defined features are needed.

2. Experimental

Fig. 1 shows a schematic diagram of the process flow for the fabrication and reactive ion etching of tantalum films. All tantalum films samples have been fabricated on a 3-in. p-type ⟨100⟩ silicon wafer (*Si-Mat Silicon Materials*). After cleaning the silicon substrate in acetone and isopropyl alcohol solvents followed by rinsing in deionized water rinse, a direct current (DC) magnetron sputtering system (*Oxford Plasmalab System 400 Sputter Coater*) has been utilised to deposit a 1-μm-thick layer of tantalum (Fig. 1a). The target material used in the sputter deposition system is 99.99% pure tantalum. Assisted by argon gas with a flow rate of 50 sccm, the sputter deposition has been performed at a pressure of 11.5 mTorr and a power of 300 W. To protect the tantalum film area that is supposed to remain unetched during and after the RIE process, a 1.5-μm-thick layer of positive photoresist (*Megaposit SPR350 - Rohm and Haas Electronic Materials*) has been served as an etching mask. Using Polos MCD Spin Coater, the resist was spun on at 2500 rpm for 1 min and soft baked at 100 °C for 1 min. A standard photolithography has been employed to pattern the photoresist mask into square shapes (Fig. 1b). The photolithography process has been conducted using a Karl Suss MA8/BA8 mask aligner. After being exposed for 7 s, developed in MF-26A for 1 min (Megaposit MF-26A developer - *Rohm and Haas Electronic Materials*), the resist has been hard baked at 115 °C for 1 min. The etching has been performed using STS Multiplex RIE System. The whole surface including the square-patterned regions is exposed to a mixture of $SiCl_4$ and Ar plasmas (Fig. 1c). Consequently, the tantalum films have

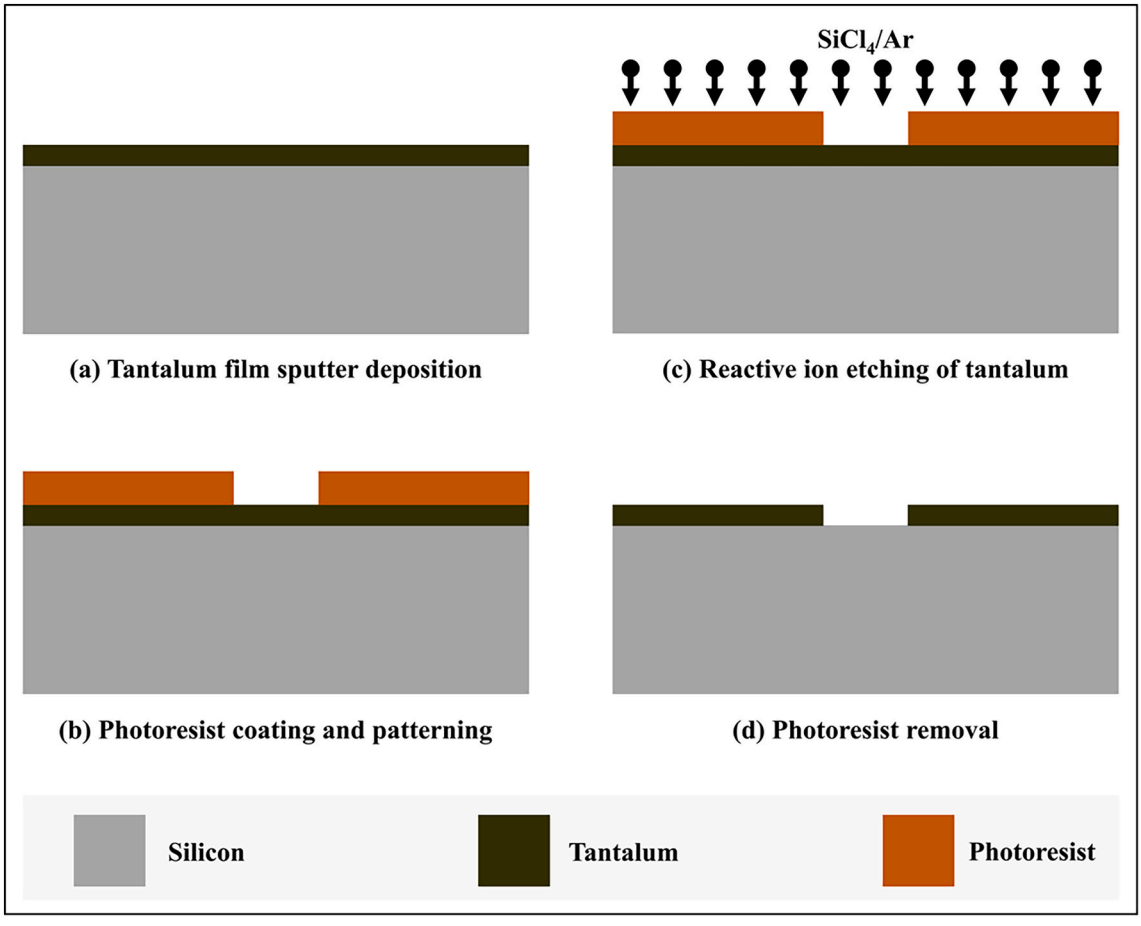

Fig. 1. Schematic illustration of fabrication and RIE process of tantalum films.

been etched using the recipe parameters presented in Table 1. After the completion of the etching, the photoresist has been removed using a solvent-based photoresist striper (acetone) (Fig. 1d). To ensure that the photoresist has been removed entirely, the samples have been subjected to O_2 ashing (Electrotech 508 Barrel Asher). The etched surface (i.e., the etching profile) has been measured using Veeco Dektak 8000 Surface Profiler. Additional measurements of the etched surface have been performed with a white light interferometer (Zygo) that has the capability to provide a non-contact and high precision 3D surface profiling. Scanning electron microscopy (SEM) and energy dispersive X-ray spectrometry (EDS) have been employed to characterise and analyse the chemical composition of etched surfaces, helping in the comprehension of the etching mechanism. It is worth pointing out that the samples have been held (i.e. the actual etching time) in the etching chamber for 15 min, thus not the whole (1-μm) tantalum layer has been etched away, (see Fig. 2d).

3. Results and discussion

Fig. 2 shows scanning electron micrographs and white light interferometry measurements of the surfaces of tantalum films etched in $SiCl_4$/Ar plasmas. Clean and anisotropic etching profiles with a vertical sidewall have been observed, evident in (Fig. 2a) and (Fig. 2b). The inset in Fig. 2b shows a zoom-in view of the etched sample where the anisotropic etching profile is clearly seen from the vertical sidewalls.

The purpose of using a white light interferometer is to ensure precise measurements of the etch depth as well as the etch profile of etched surfaces of tantalum films. An example of a typical interferometry image of a square pattern is shown in Fig. 2c. The actual profiles of the etched surfaces extracted from the interferometry measurements are depicted in Fig. 2d. The profile shows the etch depth (height) as a function of the side length (distance) of the square patterens. For nearly all patterns (50–250 μm), the etching profile has been found to be satisfactorily anisotropic (i.e., sidewall angles of ~89–89.8°). The obtained measurements from the SEM and WLI are strong evidence to exclude the scenario of isotropic etching in our devices.

3.1. Effects of etching gas composition

The first parameter to investigate its effect on the etching process of tantalum films is the flow rate of etching gases. Fig. 3 shows the dependence of the tantalum etching rate on the flow rate of $SiCl_4$ and Ar plasmas. The etching process has been conducted under a power of 60 W and a pressure of 100 mTor. In the first case, the plasma mixture ratio of $SiCl_4$/Ar are 3:1, 5:1, 7:1, 9:1 and 11:1. By holding the Ar flow rate constant at 5 sccm, the etch rate has been observed to increase significantly with the flow rate of $SiCl_4$ (see Fig. 3a). As the flow rate of $SiCl_4$ increases from 15 to 55 sccm, the etch rate has been found to increase from 23 to 62 nm/min. The increase in the etching rate is possibly related to the large number of Cl radicals generated in the plasma. As the reactive species density increases, a chemical etching occurs. Such observations are in agreement with previous etching experiments [37].

In the second case, the influence of adding Ar to the main etching gas on the etch rate has been examined. Fig. 3b represents the etch rate with respect to the flow rate of Ar under the same power (60 W) and pressure (100 mTorr) conditions while keeping the flow rate of $SiCl_4$ constant at 10 sccm. When the flow rate of Ar increases from 10 to 30 sccm (i.e. the plasma composition of Ar: $SiCl_4$ are 1:1, 2:1 and 3:1), a considerable decline in the etch rate has been observed. The reason for slower etching is possibly the dilution effect. Due to physical ion bombardment of Ar, increasing the Ar flow rate could influence the number of etching radicals produced in the plasma and thus lead to a decrease in the etching rate [37]. However, the obtained etch rate (~ 4 nm/min) seems to remain almost stable as more Ar is added. In this case, the number of active radicals become insufficient to induce etching. Such observations provide essential information on the role of Ar flow rate on tantalum etching. Importantly, the percentage of Ar in the total flow rate seems to have a limit like that observed for quartz [38]. Moreover, we have found that the etch side-wall profile is affected by the amount of Ar. The higher the flow rate, the more the profile tends to be anisotropic. Therefore, it can be concluded that it is recommended to maintain the Ar flow rate at 5–10 sccm.

From a comparison point of view, the obtained etching rate is ~23 nm/min for $SiCl_4$ 3:1 Ar (Fig. 3a), and it is ~9 nm/min for $SiCl_4$ 1:3 Ar (Fig. 3b). Under the same power and pressure magnitudes, the highest etching rate (~ 73 nm/min) has been achieved in the etching condition where the flow rates of Ar and $SiCl_4$ are equal. When compared with other materials, especially III-V semiconductors [33,39], etched in $SiCl_4$ plasma, the etching rate obtained here for tantalum can be considered relatively higher.

Table 1
Parameters for the reactive ion etching process of tantalum films.

Pressure (mTorr)	Power (W)	$SiCl_4$ flow (sccm)	Ar flow (sccm)
100	60	(15, 25, 35, 45, 55)	5
100	60	10	(10, 20, 30, 40, 50)
(30, 60, 120, 240)	60	25	5
100	(20, 40, 80, 100, 120)	25	5

3.2. Effects of power and pressure

The influence of the reactive ion etching pressure and power on tantalum etch rate is shown in Fig. 4. The results have been obtained under a constant flow rate of 25 sccm of $SiCl_4$ and 5 sccm of Ar. It has been observed that the etching rate decreases from 46 to 27 nm/min as the chamber pressure increases from 30 to 240 mTorr (Fig. 4a). Such a monotonic decrease in the etching rate is consistent with previous studies [37,39–41], which suggest that increasing the etching chamber pressure causes a reduction in the plasma density. In this case, the etching mechanism is influenced significantly by ion bombardment where the mean free path of ions generated decreases (i.e. low ion energies) with the increase of the plasma pressure [41]. It is also possible that etch by-products could be re-deposited on the etched surface which affects the etching depth of tantalum. Based on the observations shown in Fig. 4a, it appears that the chamber pressure in the RIE process is more likely to have physical etching characteristics.

In the case of varying the plasma power from 20 to 120 W while maintaining the pressure constant at 100 mTorr, the etching rate shown in Fig. 4b appears to rise slightly before increasing considerably at higher plasma powers. A surge in the etching rate (up to 113 nm/min) has been achieved as the plasma power rises from 60 to 120 W. It has been reported that such etching observations at high plasma powers are possibly due to great quantity of reactive Cl radicals and higher ion flux [37,40]. In general, the RIE plasma pressure and power appear to play a key role in changing the etchant concentrations and ion bombardment energy and thus affecting the etching process of tantalum [28].

3.3. Analysis of etched surfaces

The etch mechanism of tantalum in $SiCl_4$/Ar plasmas can be comprehended by inspecting the etched surface of tantalum. To do this, etch by-products formed on the tantalum surface after the RIE have been determined using SEM-EDS. The beam energy used in the EDS measurements was 15 keV. Fig. 5 shows the EDS spectra (profiles) and elemental composition (tables inset) of tantalum surfaces following the etching. Generally, the etched area has been observed to be mainly dominated by tantalum with a small percentage of oxygen (O) carbon

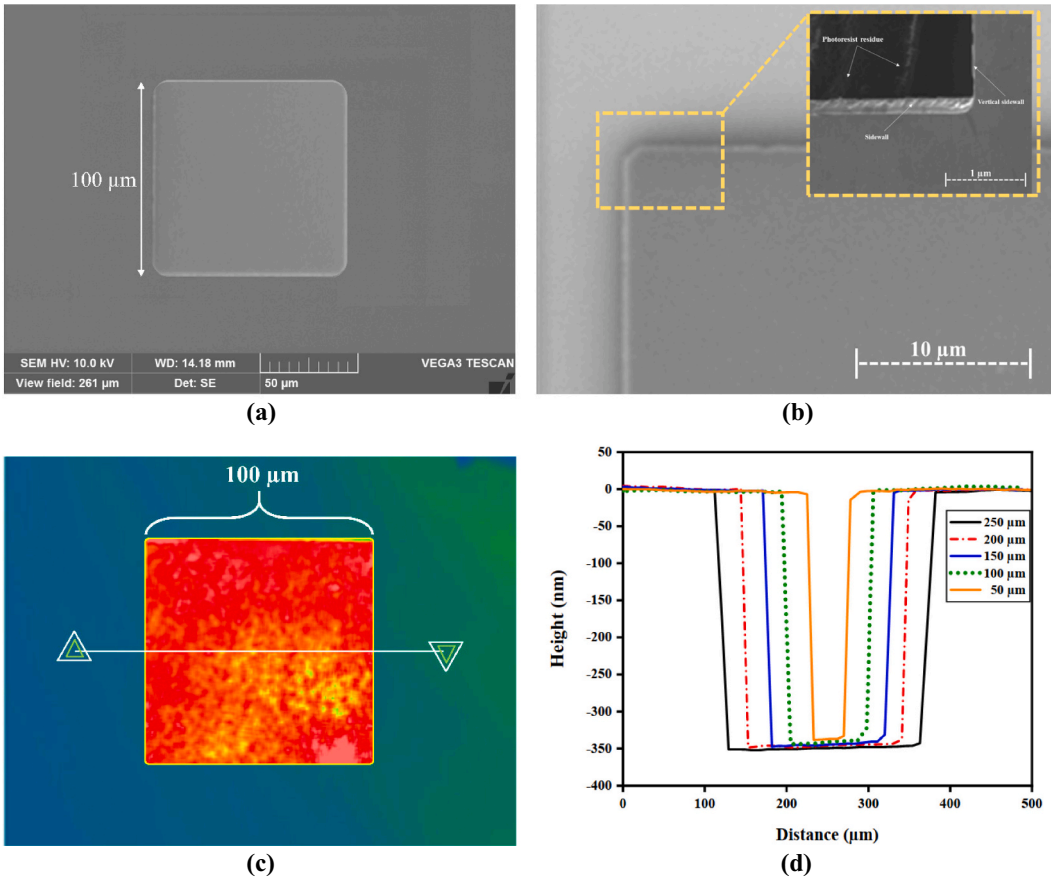

Fig. 2. SEM photographs and WLI surface profiles of tantalum etched films. (a) Top-view SEM image of a square etched pattern. (b) Top-view SEM image showing the sidewall of an etched surface. (c) Top-view WLI surface morphology. (d) Etch depth vs pattern length extracted from WLI profile.

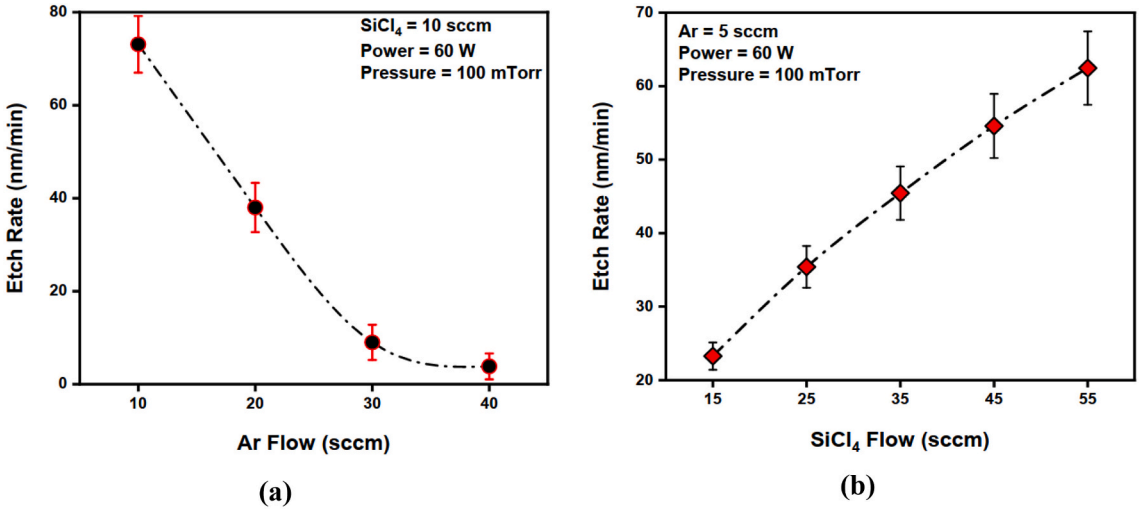

Fig. 3. Etch rate of tantalum as a function of a flow rate of etching gases of (a) $SiCl_4$ and (b) Ar. Etching parameters of power (60 W) and pressure (100 mTorr) have been held constant during the RIE.

(C) and chlorine (Cl). Oxide peaks suggest the formation of tantalum oxide (Ta_xO_y). From the atomic percentage of oxygen presented in the tables inset in Fig. 5, it is believed that tantalum pentoxide (Ta_2O_5) has been formed. It is highly possible that the sputter-deposited tantalum films have been oxidised during the sputtering or due to exposure to the atmospheric environment. This native oxide can be removed by physical sputtering during the RIE process.

It is worthwhile to mention that the absence of silicon peaks in the EDS data is because of the fact that EDS is not sensitive to surface. Based on that, we would exclude the reported scenario [36] which claimed that a layer of silicon dioxide (SiO_2) might be formed due to a reaction in the etching chamber between oxygen and a silicon precursor resulting from $SiCl_4$. Therefore, the appearance of oxygen peaks suggests that the oxide layer has been created after the etching. Following the removal of

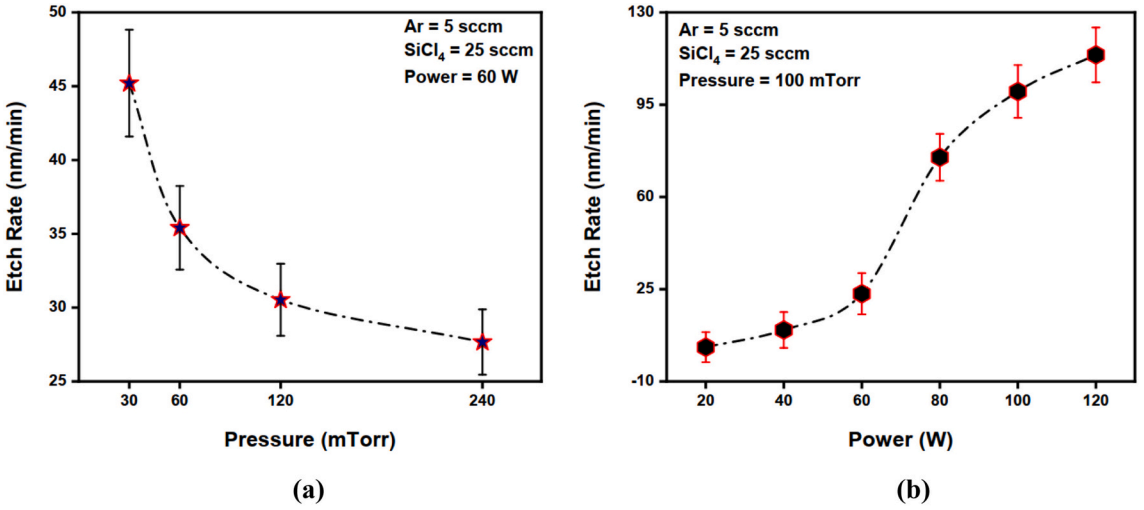

Fig. 4. Etch rate of tantalum as a function of plasma (a) pressure and (b) power. The flow rates of etching gases of $SiCl_4$ and Ar have been held constant at 25 sccm and 5 sccm, respectively.

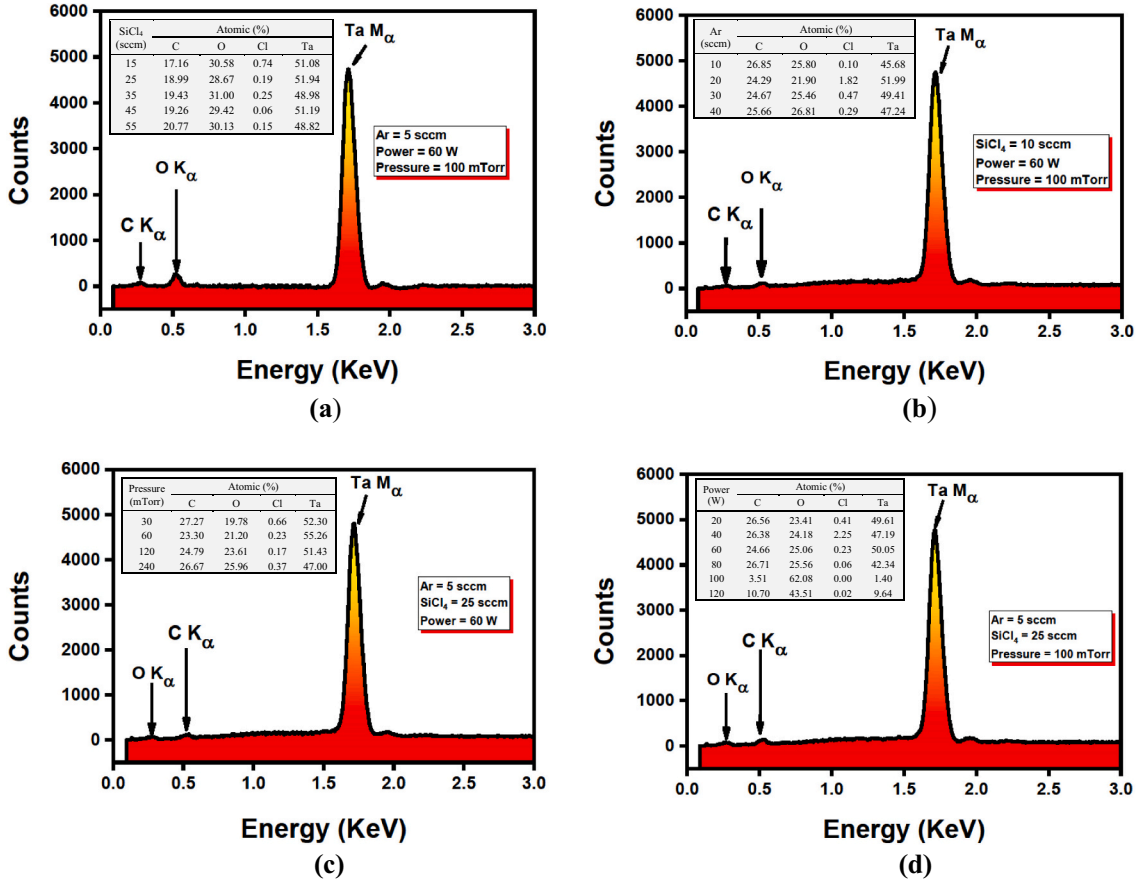

Fig. 5. EDS spectra of RIE etched surfaces of tantalum films in $SiCl_4$/Ar plasmas. Each spectrum represents measurements of etched film samples with respect to (a) $SiCl_4$ flow rate, (b) Ar flow rate, (c) pressure change and (d) power change. Insets are tables showing the chemical composition in atomic (%) of the etched surfaces.

the thin oxide layer, a reaction could occur between chlorine species and tantalum resulting in the formation of volatile etch products such as tantalum chloride ($TaCl_x$). Nevertheless, the small percentage of chlorine depicted in the tables inset in Fig. 5 suggests that tantalum chloride has been formed on the surface. Although carbon has not been used in etching, carbon peaks have been detected. The source of this carbon could be attributed to contamination induced during the RIE process [36,42,43].

4. Conclusions

An enhanced and controllable dry etching process of tantalum can be achieved by exploring the main factors that have a major impact on etching mechanism. Tantalum films of thickness of 1 μm sputter-

deposited on a silicon substrate and masked with photoresist have been etched in a reactive ion etching system using $SiCl_4$ and Ar plasmas. The etching process presented in this work is intended to provide a comprehensive investigation on the effect of different etching parameters on the etching of tantalum. The etching rate has been studied with respect to etching gases ratio of $SiCl_4$/Ar, a chamber pressure from 30 to 240 mTorr and a plasma power ranging from 20 to 120 W. A significant increase in the etching rate has been observed when the flow rate of $SiCl_4$ and plasma power increase. It has been found that adding more Ar to the main etching gas or increasing the chamber pressure leads to a decline in the etching rate. Based on the outcomes obtained from this work, an optimum etch recipe for etching tantalum films can be determined.

Declaration of Competing Interest

We confirm that this work is original and has not been published elsewhere nor is it currently under consideration for publication elsewhere. None of the authors of this paper has a financial or personal relationship with other people or organizations that could inappropriately influence or bias the content of the paper.

Acknowledgments

The authors would like to acknowledge Camelia Dunare and Karina Jeronimo Martinez for their technical assistance in EDS measurements.

References

[1] C.L. Briant, New applications for refractory metals, JOM. 52 (2000) 36, https://doi.org/10.1007/s11837-000-0098-9.
[2] G. Abadias, J.J. Colin, D. Tingaud, P. Djemia, L. Belliard, C. Tromas, Elastic properties of α- and β-tantalum thin films, Thin Solid Films 688 (2019), 137403, https://doi.org/10.1016/j.tsf.2019.06.053.
[3] S. Shiri, C. Zhang, A. Odeshi, Q. Yang, Growth and characterization of tantalum multilayer thin films on CoCrMo alloy for orthopedic implant applications, Thin Solid Films 645 (2018) 405–408, https://doi.org/10.1016/j.tsf.2017.11.017.
[4] A.K. Al-mashaal, G. Wood, E. Mastropaolo, R. Cheung, Electrostatically driven long-microbeams for low-frequency applications, Electron. Lett. 54 (2018) 372–374, https://doi.org/10.1049/el.2017.4534.
[5] A. Al-Mashaal, E. Mastropaolo, A. Bunting, C. Dunare, R. Cheung, Fabrication and characterisation of suspended microstructures of tantalum, J. Micromech. Microeng. 27 (2017), 015020, https://doi.org/10.1088/0960-1317/27/1/015020.
[6] A. Al-Mashaal, A. Bunting, R. Cheung, Evaluation of residual stress in sputtered tantalum thin-film, Appl. Surf. Sci. 371 (2016) 571–575, https://doi.org/10.1016/j.apsusc.2016.02.236.
[7] E. Mastropaolo, R. Latif, E. Grady, R. Cheung, Control of stress in tantalum thin films for the fabrication of 3D MEMS structures, J. Vac. Sci. Technol. B Microelectron. Nanom. Struct. 31 (2013) 06FD02, https://doi.org/10.1116/1.4824697.
[8] R. Latif, E. Mastropaolo, A. Bunting, R. Cheung, T. Koickal, A. Hamilton, M. Newton, L. Smith, Low frequency tantalum electromechanical systems for biomimetical applications, J. Vac. Sci. Technol. B, Nanotechnol. Microelectron. Mater. Process. Meas. Phenom. 29 (2011) 06FE05, https://doi.org/10.1116/1.3662408.
[9] R. Latif, E. Mastropaolo, A. Bunting, R. Cheung, T. Koickal, A. Hamilton, M. Newton, L. Smith, Microelectromechanical systems for biomimetical applications, J. Vac. Sci. Technol. B, Nanotechnol. Microelectron. Mater. Process. Meas. Phenom. 28 (2010) C6N1-C6N6, https://doi.org/10.1116/1.3504892.
[10] V. Rinnerbauer, J.J. Senkevich, J.D. Joannopoulos, M. Soljačić, I. Celanovic, R. R. Harl, B.R. Rogers, Low emissivity high-temperature tantalum thin film coatings for silicon devices, J. Vac. Sci. Technol. A Vacuum, Surfaces, Film. 31 (2013), 011501, https://doi.org/10.1116/1.4766295.
[11] L.L. Liu, J. Xu, X. Lu, P. Munroe, Z.H. Xie, Electrochemical corrosion behavior of Nanocrystalline β-ta coating for biomedical applications, ACS Biomater. Sci. Eng. 2 (2016) 579–594, https://doi.org/10.1021/acsbiomaterials.5b00552.
[12] L. Gladczuk, A. Patel, C.S. Paur, M. Sosnowski, Tantalum films for protective coatings of steel, Thin Solid Films 467 (2004) 150–157, https://doi.org/10.1016/j.tsf.2004.04.041.
[13] D.H. Kim, J.S. Park, D. Kang, T.Y. Seong, A tantalum diffusion barrier layer for improving the output performance of AlGaInP-based light-emitting diodes, Jpn. J. Appl. Phys. 55 (2016), 032102, https://doi.org/10.7567/JJAP.55.032102.
[14] S. Balachandran, K.T. Hartwig, D.C. Baars, S.N. Mathaudhu, T.R. Bieler, T. Pyon, R. E. Barber, Fabrication of tantalum sheet for superconductor diffusion barriers, in, IEEE Trans. Appl. Supercond. (2009) 2606–2609, https://doi.org/10.1109/TASC.2009.2018153.
[15] K.A. De Souza, A. Robin, Electrochemical behavior of titanium-tantalum alloys in sulfuric acid solutions, Mater. Corros. 55 (2004) 853–860, https://doi.org/10.1002/maco.200303792.
[16] Stephen D. Cramer, J. Bernard, S. Covino (Eds.), Corrosion of Tantalum and Tantalum Alloys, in: Corros. Mater., ASM International, 2018, pp. 337–353, https://doi.org/10.31399/asm.hb.v13b.a0003825.
[17] T.B. Tripp, J. Eckert, Tantalum and tantalum compounds, in: Kirk-Othmer Encycl. Chem. Technol., John Wiley & Sons, Inc, Hoboken, NJ, USA, 2000, https://doi.org/10.1002/0471238961.2001142020180916.a01.
[18] K. Rydzynski, D. Pakulska, Vanadium, niobium, and tantalum, in: Patty's Toxicol., John Wiley & Sons, Inc, Hoboken, NJ, USA, 2012, pp. 511–564, https://doi.org/10.1002/0471435139.tox037.pub2.
[19] S. Sood, R. Peelamedu, K.B. Sundaram, E. Dein, R.M. Todi, Wet etching of sputtered tantalum thin films in NaOH and KOH based solutions, J. Mater. Sci. Mater. Electron. 18 (2007) 535–539, https://doi.org/10.1007/s10854-006-9053-z.
[20] H. Li, Microfabrication techniques for producing freestanding multi-dimensional microstructures, Microsyst. Technol. 22 (2016) 223–237, https://doi.org/10.1007/s00542-015-2720-3.
[21] H. Zhu, M. Holl, T. Ray, S. Bhushan, D.R. Meldrum, Characterization of deep wet etching of fused silica glass for single cell and optical sensor deposition, J. Micromech. Microeng. 19 (2009) 65013, https://doi.org/10.1088/0960-1317/19/6/065013.
[22] A. Picard, G. Turban, Plasma etching of refractory metals (W, Mo, Ta) and silicon in SF6 and SF6-O2. An analysis of the reaction products, Plasma Chem. Plasma Process. 5 (1985) 333–351, https://doi.org/10.1007/BF00566008.
[23] M. Nakaishi, K. Sugishima, Precise reactive ion etching of ta absorber on x-ray masks, Jpn. J. Appl. Phys. 30 (1991) 3065–3069, https://doi.org/10.1143/JJAP.30.3065.
[24] M. Nakaishi, M. Yamada, K. Kondo, M. Yamabe, K. Sugishima, Anomalous etching residues of sputter-deposited ta upon reactive ion etching using chlorine-based plasmas, Jpn. J. Appl. Phys. 31 (1992) L1625–L1627, https://doi.org/10.1143/JJAP.31.L1625.
[25] R. Hsiao, D. Miller, T. Lin, N. Robertson, Tantalum plasma etching with minimum effect on underlying nickel-iron thin film, Thin Solid Films 304 (1997) 381–385, https://doi.org/10.1016/S0040-6090(97)00190-9.
[26] T.P. Chow, A.J. Steckl, Plasma etching of refractory gates for VLSI applications, J. Electrochem. Soc. 131 (1984) 2325–2335, https://doi.org/10.1149/1.2115251.
[27] V.J. Tu, J.Y. Jeong, A. Schütze, S.E. Babayan, G. Ding, G.S. Selwyn, R.F. Hicks, Tantalum etching with a nonthermal atmospheric-pressure plasma, J. Vac. Sci. Technol. A Vacuum, Surfaces, Film. 18 (2000) 2799–2805, https://doi.org/10.1116/1.1310652.
[28] Y. Kuo, Reactive ion etching of sputter deposited tantalum with Cf4, Cf3Cl, and CHF3, Jpn. J. Appl. Phys. 32 (1993) 179–185, https://doi.org/10.1143/JJAP.32.179.
[29] Y. Kuo, Reactive ion etching of sputter deposited tantalum oxide and its etch selectivity to tantalum, J. Electrochem. Soc. 139 (1992) 579, https://doi.org/10.1149/1.2069261.
[30] R. Hsiao, D. Miller, Etching of tantalum in fluorine-containing high density plasmas, J. Electrochem. Soc. 143 (1996) 3266–3270, https://doi.org/10.1149/1.1837195.
[31] V. Rinnerbauer, S. Ndao, Y. Xiang Yeng, J.J. Senkevich, K.F. Jensen, J. D. Joannopoulos, M. Soljačić, I. Celanovic, R.D. Geil, Large-area fabrication of high aspect ratio tantalum photonic crystals for high-temperature selective emitters, J. Vac. Sci. Technol. B, Nanotechnol. Microelectron. Mater. Process. Meas. Phenom. 31 (2013), 011802, https://doi.org/10.1116/1.4771901.
[32] J.H. Choi, S.M. Hwang, J.Y. Lee, A.A. Garay, C.W. Chung, Highly anisotropic etching of Ta thin films using high density plasmas of halogen based gases, Vacuum. 133 (2016) 18–24, https://doi.org/10.1016/j.vacuum.2016.08.003.
[33] S. Golka, S. Schartner, W. Schrenk, G. Strasser, Low bias reactive ion etching of GaAs with a SiCl[sub 4]/N[sub 2]/O[sub 2] time-multiplexed process, J. Vac. Sci. Technol. B Microelectron. Nanom. Struct. 25 (2007) 839, https://doi.org/10.1116/1.2737439.
[34] S. Hönl, H. Hahn, Y. Baumgartner, L. Czornomaz, P. Seidler, Highly selective dry etching of GaP in the presence of AlxGa1-xP with a SiCl4/SF6 plasma, J. Phys. D. Appl. Phys. 51 (2018), 185203, https://doi.org/10.1088/1361-6463/aab8b7.
[35] Y. Kuo, Reactive ion etch processes for amorphous silicon thin film transistors, J. Electrochem. Soc. 141 (1994) 502, https://doi.org/10.1149/1.2054754.
[36] H. Shimada, K. Maruyama, Highly selective etching of tantalum electrode to thin gate dielectrics usine SiCI4-NF3 gas mixture plasma, in: Japanese J. Appl. Physics, Part 1 Regul. Pap. Short Notes Rev. Pap., Japan Society of Applied Physics, 2004, pp. 1768–1772, https://doi.org/10.1143/JJAP.43.1768.
[37] C.C. Kao, H.W. Huang, J.Y. Tsai, C.C. Yu, C.F. Lin, H.C. Kuo, S.C. Wang, Study of dry etching for GaN and InGaN-based laser structure using inductively coupled plasma reactive ion etching, Mater. Sci. Eng. B Solid-State Mater. Adv. Technol. 107 (2004) 283–288, https://doi.org/10.1016/j.mseb.2003.11.023.
[38] H. Chen, C. Fu, An investigation into the characteristics of deep reactive ion etching of quartz using SU-8 as a mask, J. Micromech. Microeng. 18 (2008), 105001, https://doi.org/10.1088/0960-1317/18/10/105001.
[39] X. Li, H. Zhou, R.J.W. Hill, P. Longo, M. Holland, I.G. Thayne, Dry etching device quality high-κ GaxGdyOz gate oxide in SiCl4 chemistry for low resistance ohmic contact realisation in fabricating III-V MOSFETs, Microelectron. Eng. 87 (2010) 1587–1589, https://doi.org/10.1016/j.mee.2009.11.011.
[40] A.P. Shah, A.A. Rahman, A. Bhattacharya, ICP-RIE etching of polar, semi-polar and non-polar AlN: comparison of Cl2/Ar and Cl2/BCl3/Ar plasma chemistry and surface pretreatment, Semicond. Sci. Technol. 30 (2015), 015021, https://doi.org/10.1088/0268-1242/30/1/015021.

[41] E. Mastropaolo, A.M. Gundlach, C. Fragkiadakis, P.B. Kirby, R. Cheung, Reactive ion etching of zinc oxide (ZnO) in SiCl4 based plasmas, Electron. Lett. 43 (2007) 1467–1469, https://doi.org/10.1049/el:20072977.
[42] P. Kaspar, P. Škarvada, V. Holcman, L. Grmela, Characterization of argon etched Ta2O5 thin films, Appl. Phys. A Mater. Sci. Process. 125 (2019) 820, https://doi.org/10.1007/s00339-019-3134-3.
[43] I. Adesida, A. Mahajan, E. Andideh, M.A. Khan, D.T. Olsen, J.N. Kuznia, Reactive ion etching of gallium nitride in silicon tetrachloride plasmasa, Appl. Phys. Lett. 63 (1993) 2777–2779, https://doi.org/10.1063/1.110331.